*Supporting Information*

# A General Synthetic Approach for Integrated Nanocatalysts of Metal-Silica@ZIFs

Baojuan Xi,[a,b] Ying Chuan Tan,[a] and Hua Chun Zeng [a,*]

[a]*Department of Chemical and Biomolecular Engineering, Faculty of Engineering, National University of Singapore, 10 Kent Ridge Crescent, Singapore 119260*

[b]*School of Chemistry and Chemical Engineering, Shandong University No 27 Shandananlu, Jinan, Shandong, 250100, China*

**Email: chezhc@nus.edu.sg*

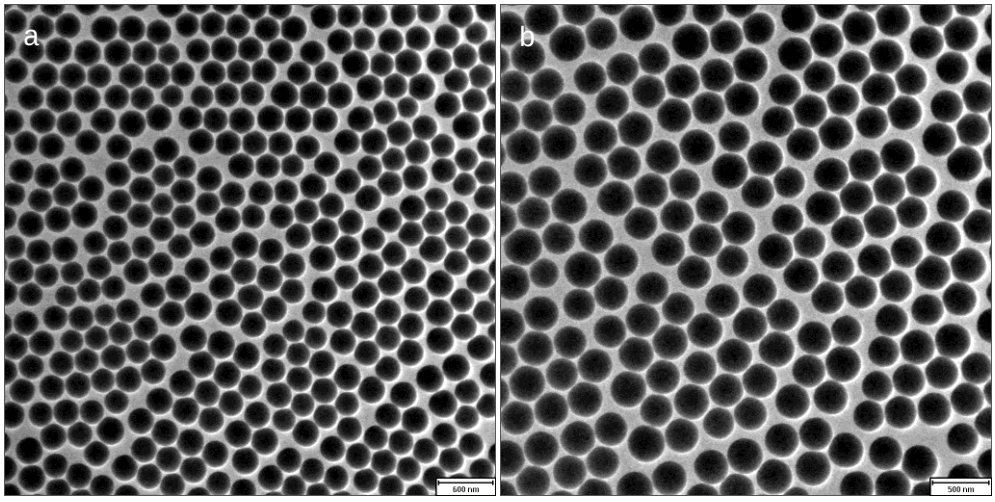


**Figure S1** (a,b) TEM images (at different magnifications) of monodisperse Stöber $SiO_2$ spheres.

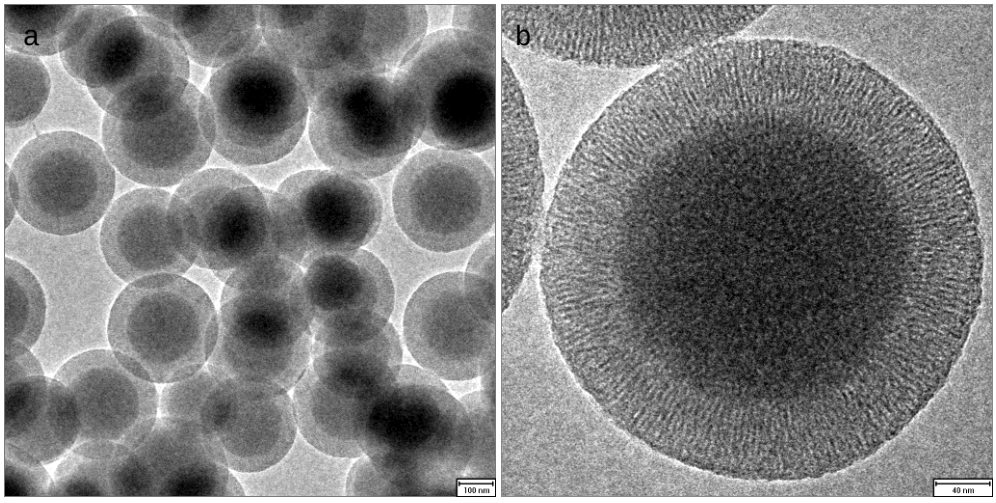


**Figure S2** (a,b) TEM images (at different magnifications) of mesoporous $SiO_2$ spheres synthesized at 120 °C for 12 h.

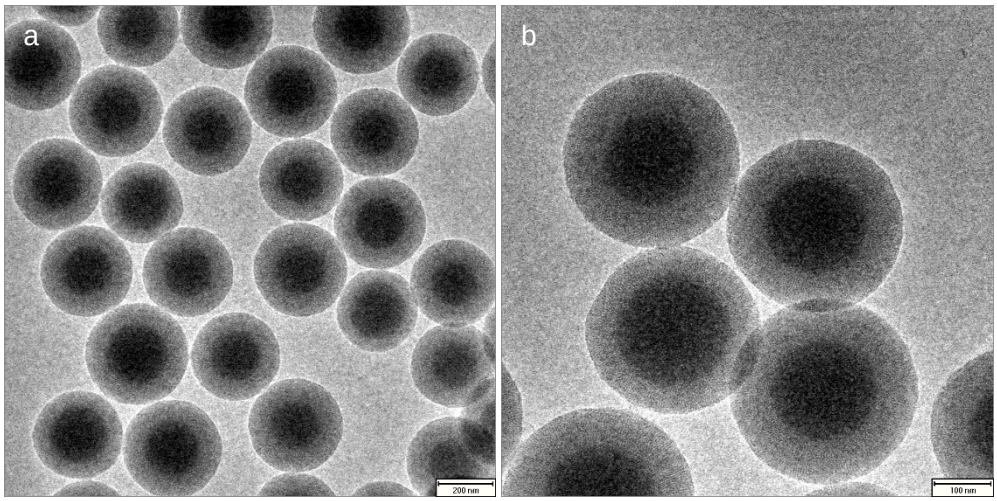


**Figure S3** (a,b) TEM images (at different magnifications) of mesoporous $SiO_2$ spheres synthesized hydrothermally at 160 °C for 12 h.

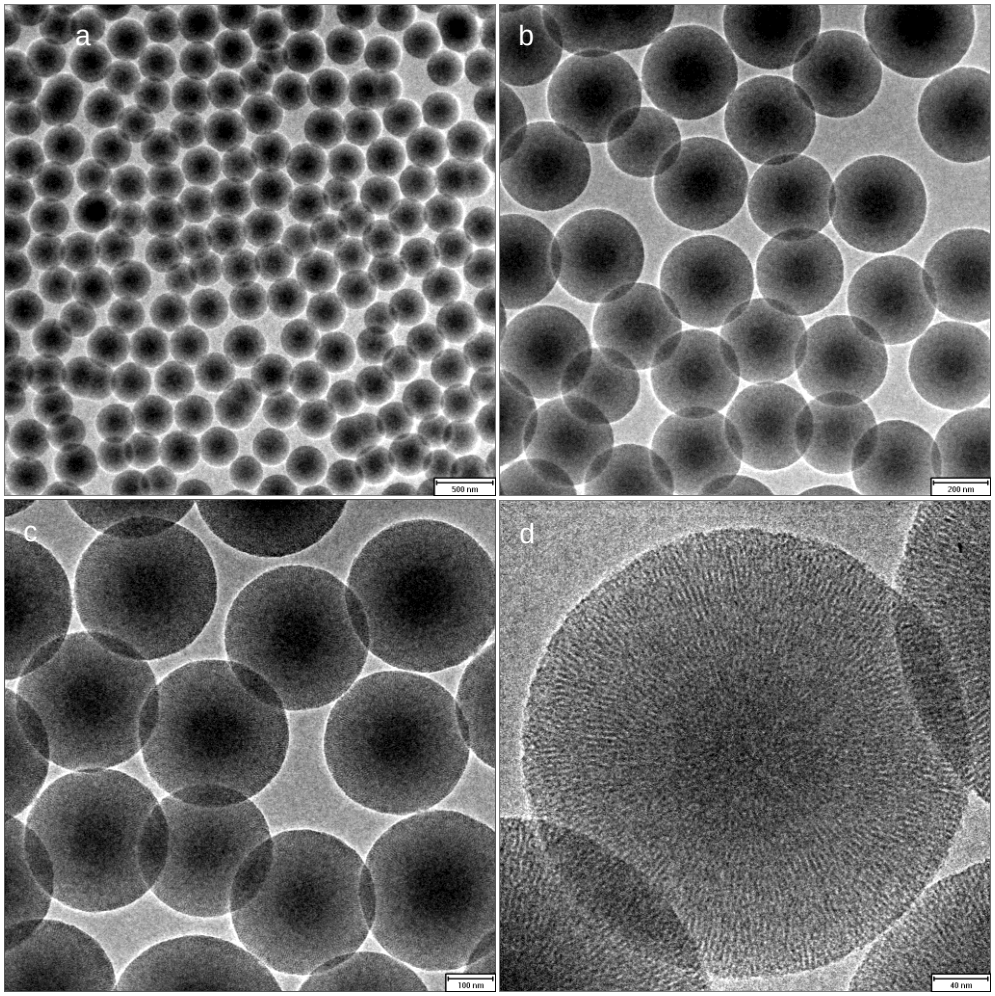


**Figure S4** (a−d) TEM images (at different magnifications) of mesoporous $SiO_2$ spheres obtained with 0.2 g CTAB (concentration of 18.3 mM) at 160 °C for 12 h.

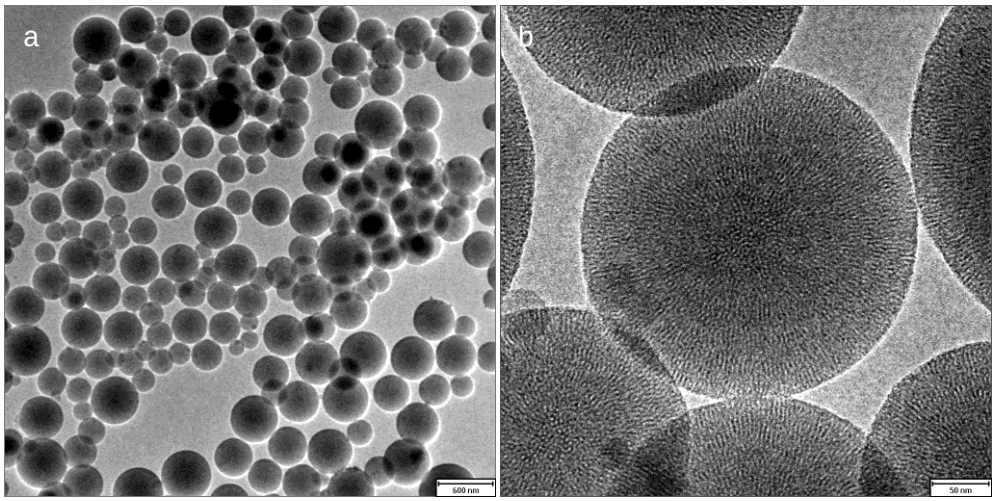


**Figure S5** (a,b) TEM images (at different magnifications) of mesoporous $SiO_2$ spheres obtained with 5.2 mM CTAB at 180 °C for 12 h.

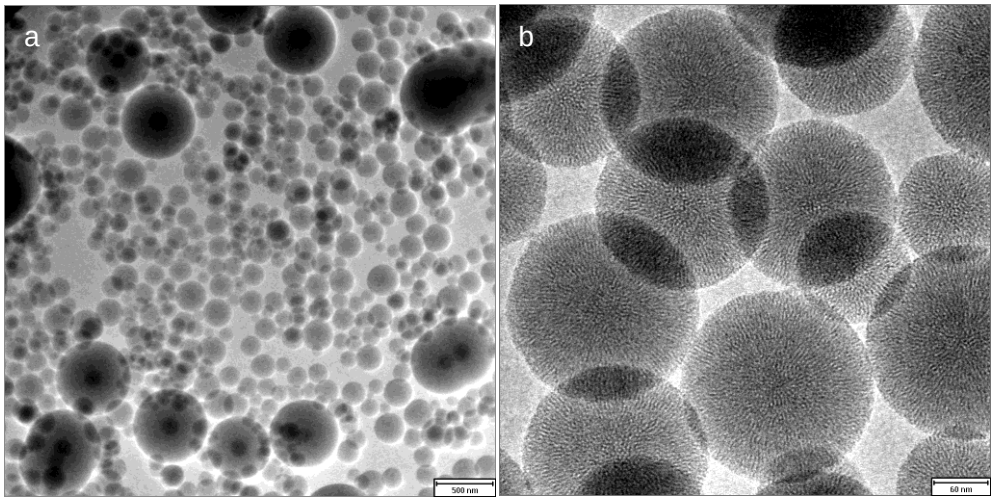


**Figure S6** (a,b) TEM images (at different magnifications) of mesoporous $SiO_2$ spheres obtained with 18.3 mM CTAB at 180 °C for 12 h.

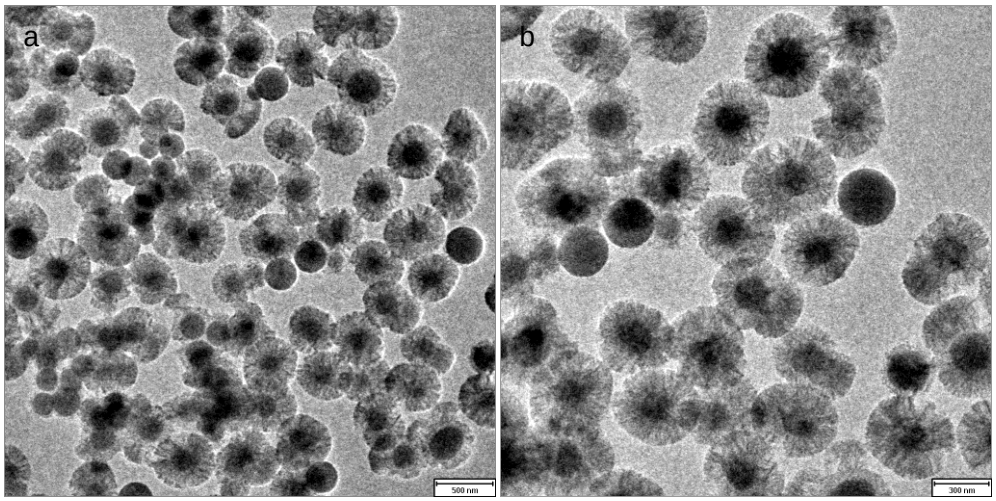


**Figure S7** (a,b) TEM images (at different magnifications) of pore-expanded mesoporous $SiO_2$ at 140 °C for 12 h with addition of 0.25 mL DMDA.

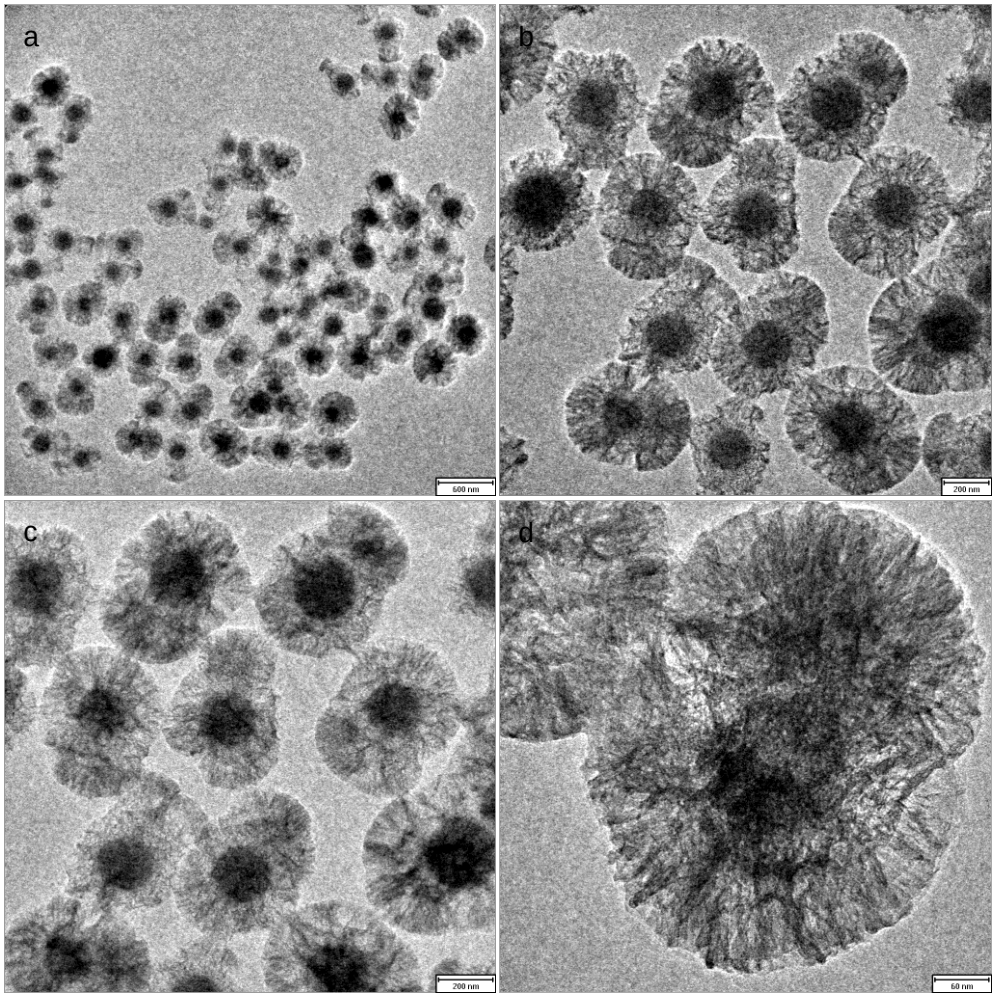


**Figure S8** (a−d) TEM images (at different magnifications) of pore-expanded mesoporous $SiO_2$ at 140 °C for 12 h with addition of 0.5 mL of DMDA.

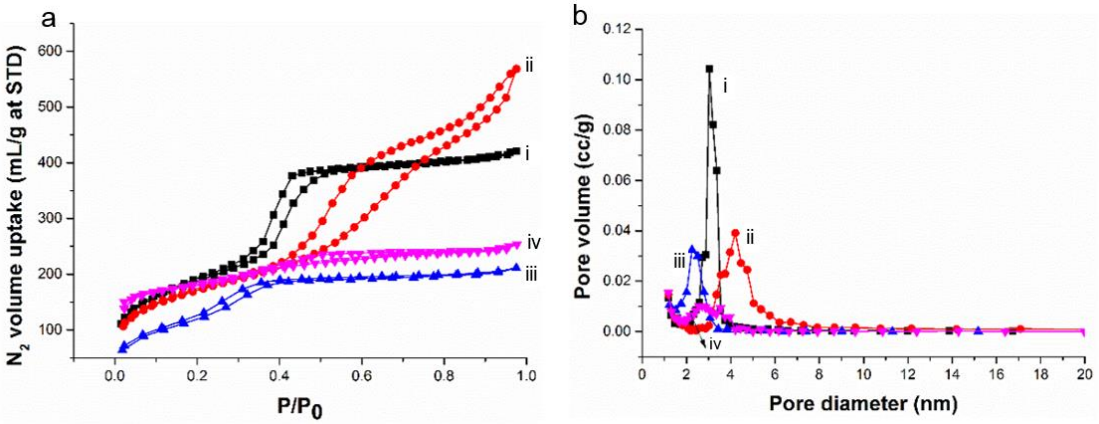


**Figure S9** (a) Isothermal nitrogen adsorption-desorption loops and (b) corresponding BJH pore size distribution of (i) normal MCM-41 $SiO_2$, (ii) pore-expanded mesoporous $SiO_2$, (iii) Pd-*m*$SiO_2$, and (iv) Pd-*m*$SiO_2$@ZIF-8.

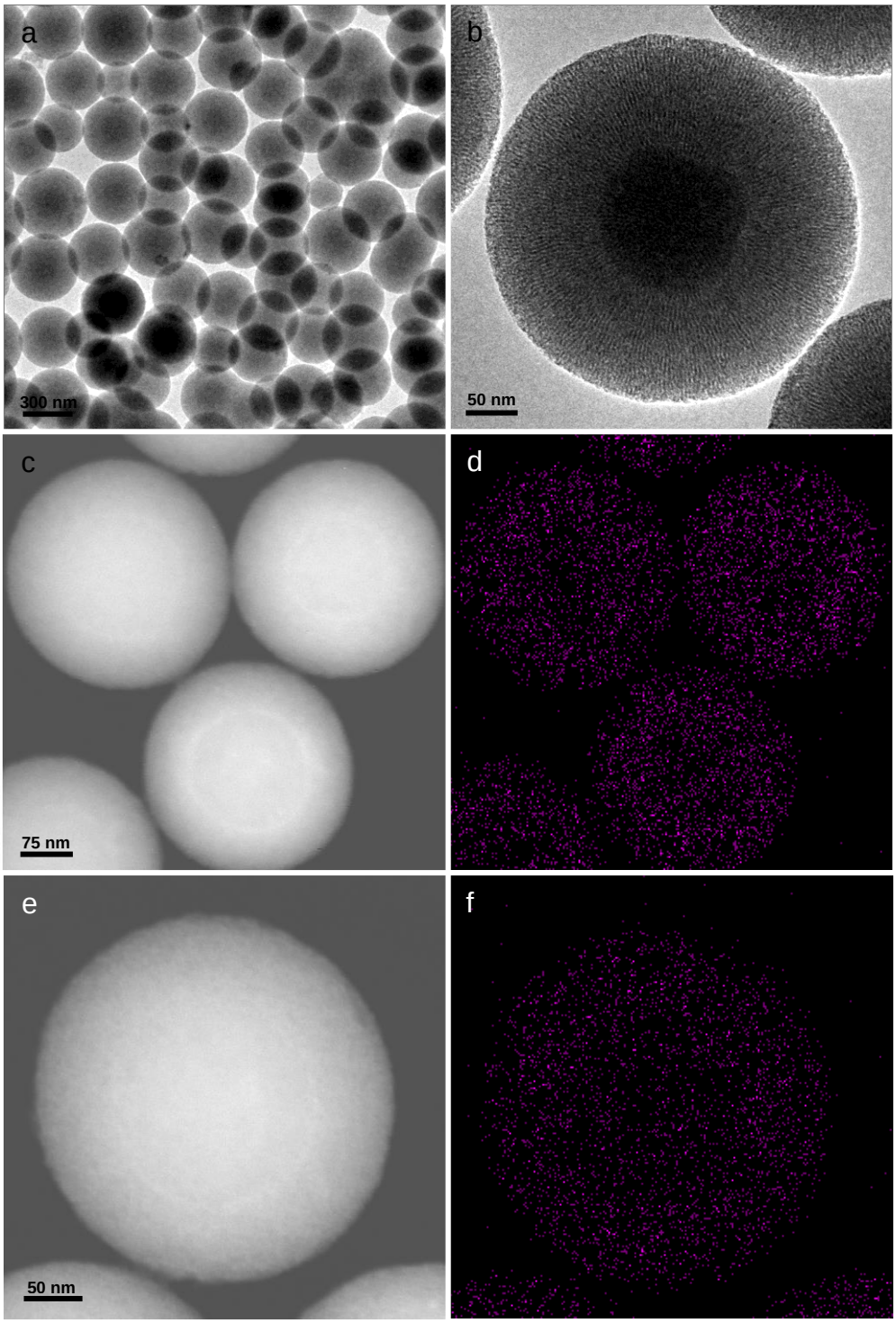


**Figure S10** (a,b) TEM images (at different magnifications), (c,e) HAADF-STEM, and (d,f) corresponding Pt mapping images of Pt-*m*$SiO_2$ spheres with $K_2PtCl_4$ aqueous solution as precursor.

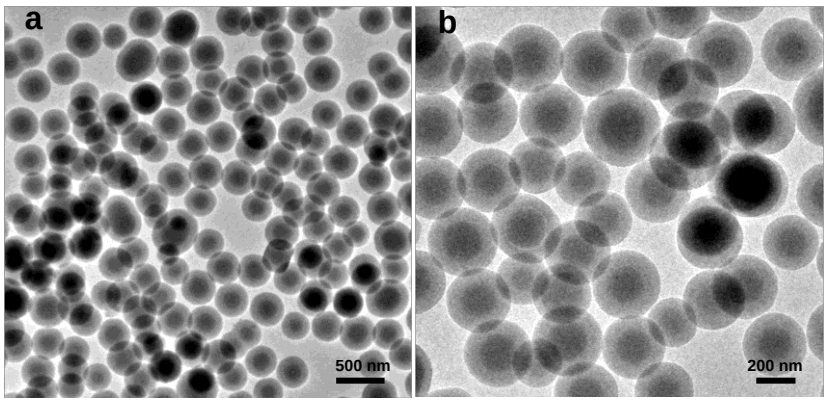


**Figure S11** (a,b) TEM images (at different magnifications) of monodisperse Pd-*m*$SiO_2$ spheres with $Pd(OAc)_2$ dissolved in acetone.

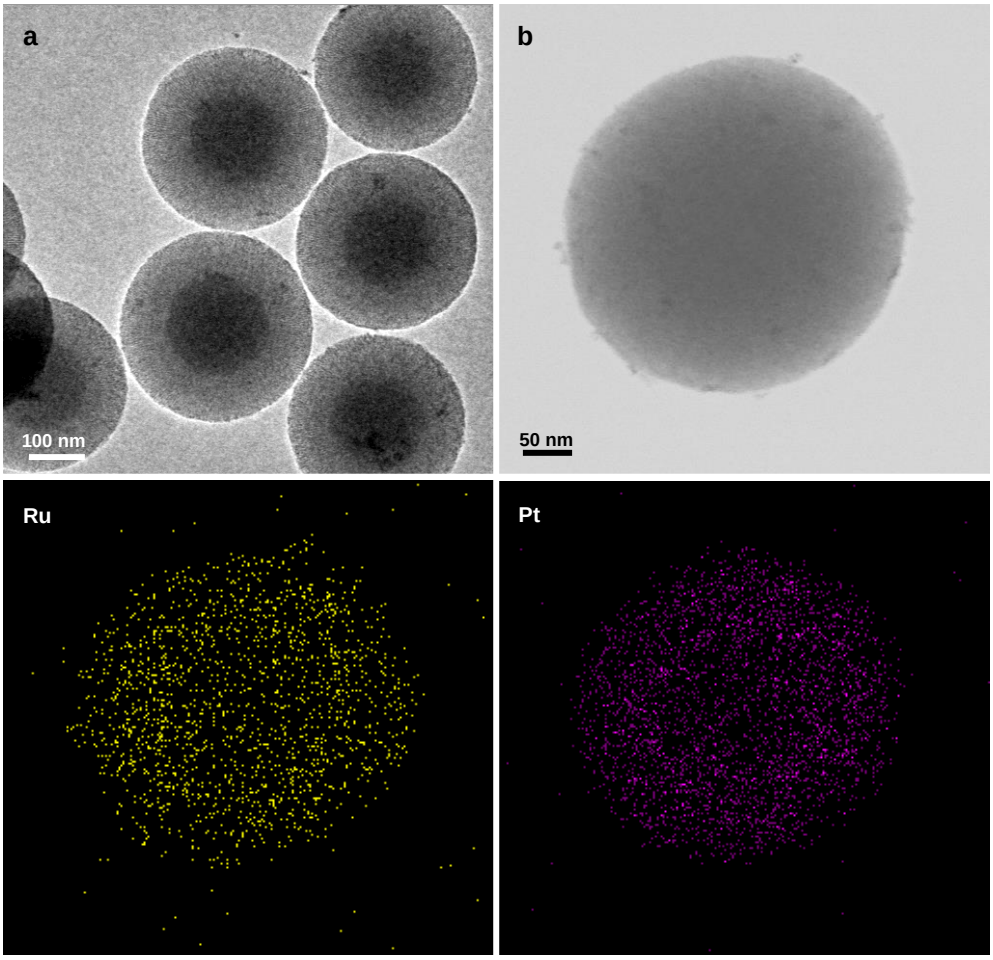


**Figure S12** (a) TEM image of monodisperse $Ru_{47}Pt_{53}$-*m*$SiO_2$ spheres, and (b) STEM image and its related mapping images (Ru and Pt) of a typical sphere.

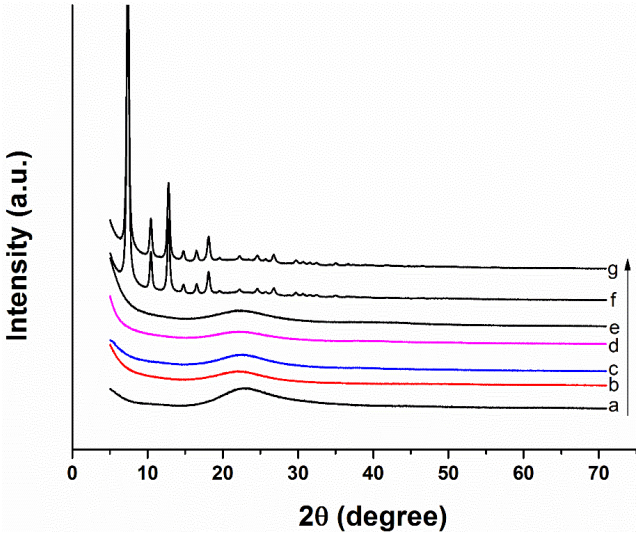


**Figure S13** XRD patterns of (a) mesoporous $SiO_2$ spheres, (b) Ru-*m*$SiO_2$, (c) Ag-*m*$SiO_2$, (d) Pd-*m*$SiO_2$, (e) RuPt-*m*$SiO_2$, and Pd-*m*$SiO_2$@ZIF-8 prepared in methanol (f) before and (g) after calcination.

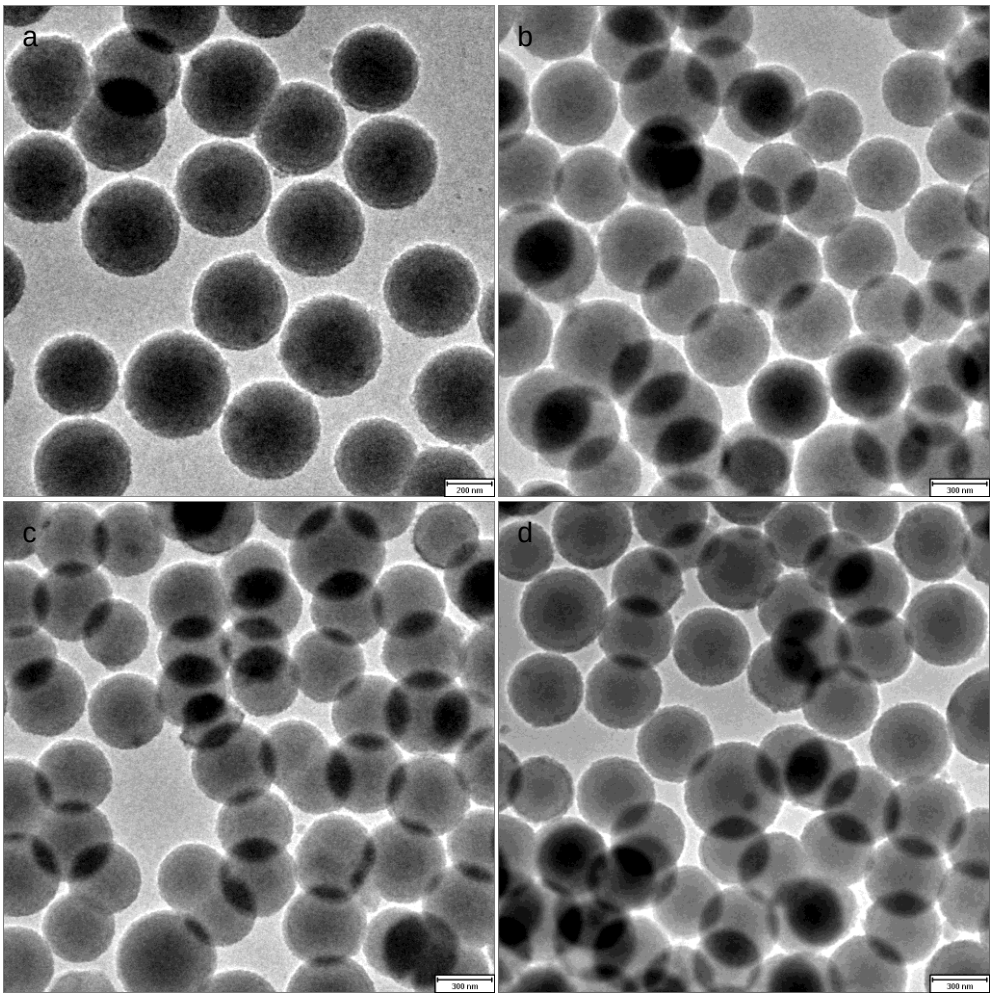


**Figure S14** TEM images of Pt-*m*$SiO_2$@ZIF-8 fabricated with different amounts of PVP while keeping other conditions identical: (a) 0.01 g, (b) 0.02 g, (c) 0.03 g, and (d) 0.04 g.

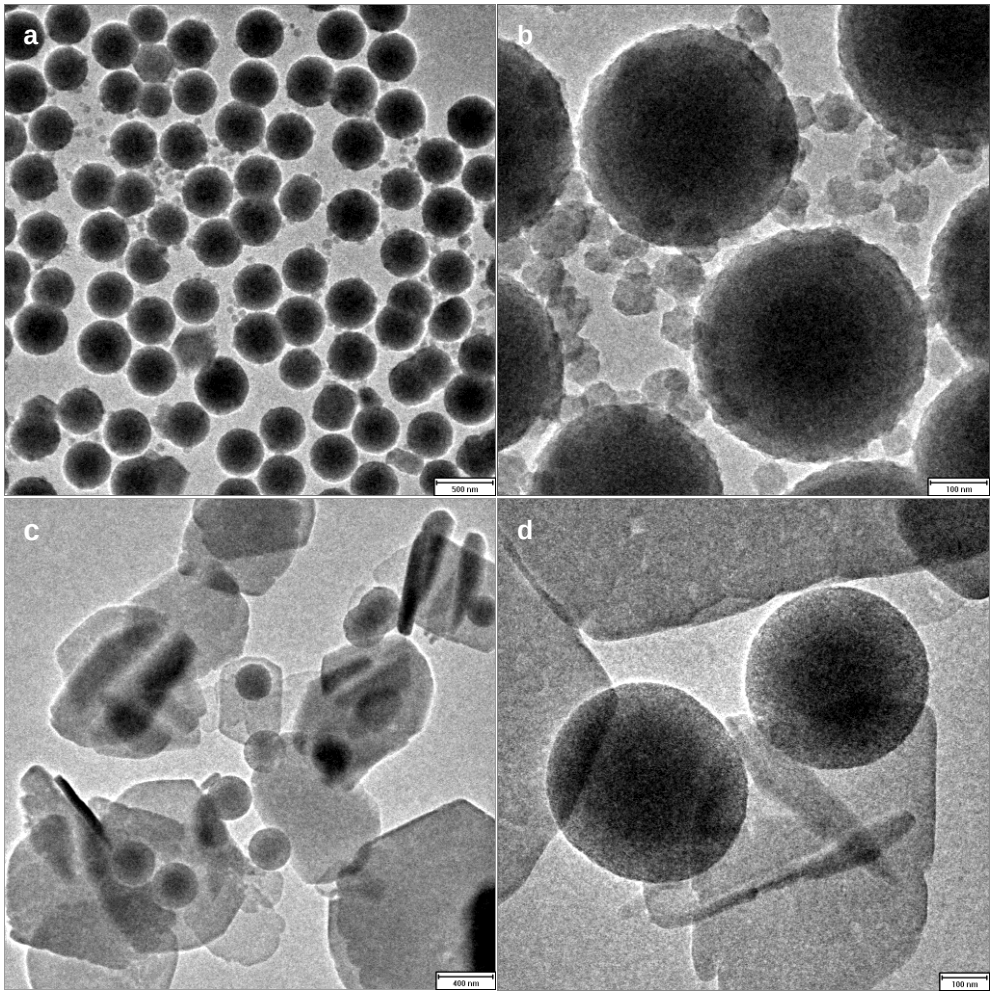


**Figure S15** TEM images of Pt-*m*$SiO_2$/ZIF-8 prepared with different precursors in the presence of 0.02 g PVP: (a,b) 2.5 mL of 0.0672 M $Zn(NO_3)_2$ (0.168 mmol) and 1.1 mmol of 2-MeIM, and (c,d) 3.75 mL of 0.0672 M $Zn(NO_3)_2$ (0.252 mmol ) and 1.65 of mmol 2-MeIM.

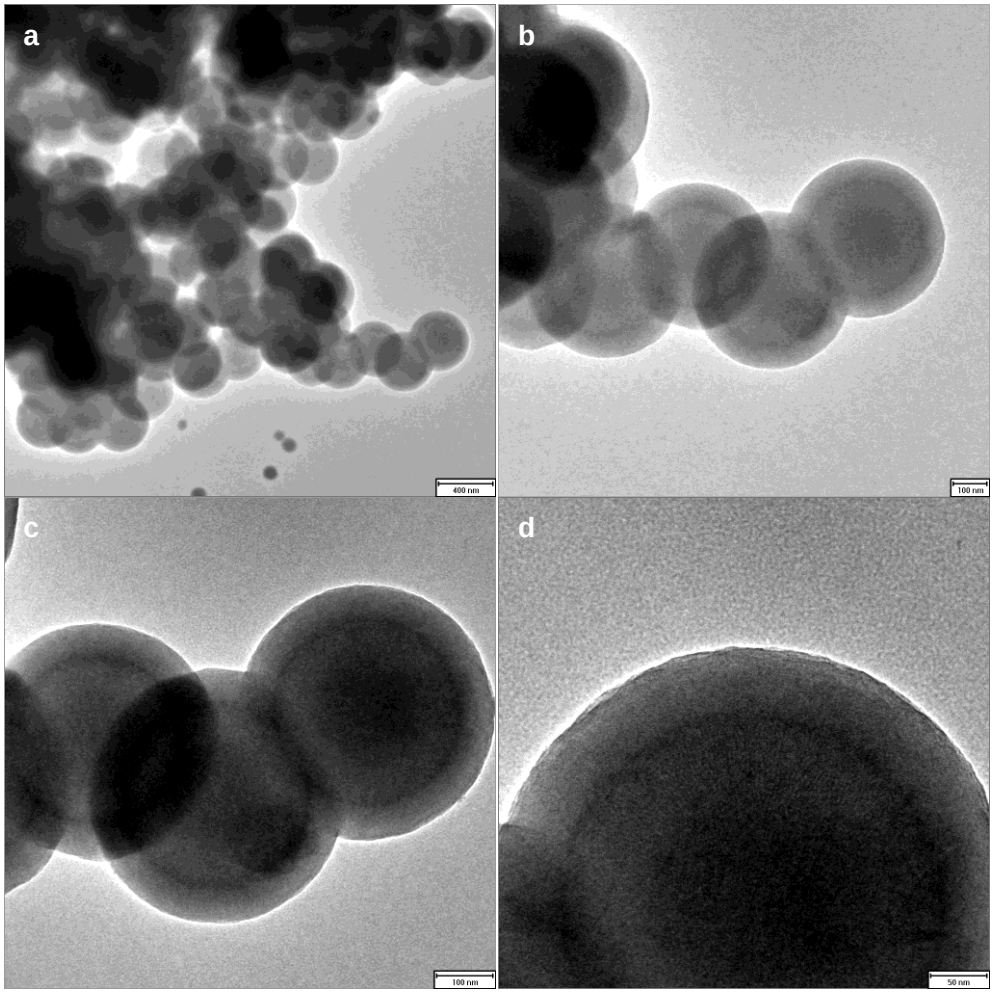


**Figure S16** (a−d) TEM images (at different magnifications) of Pt-*m*$SiO_2$ after coating with ZIF-8 fabricated without the addition of PVP.

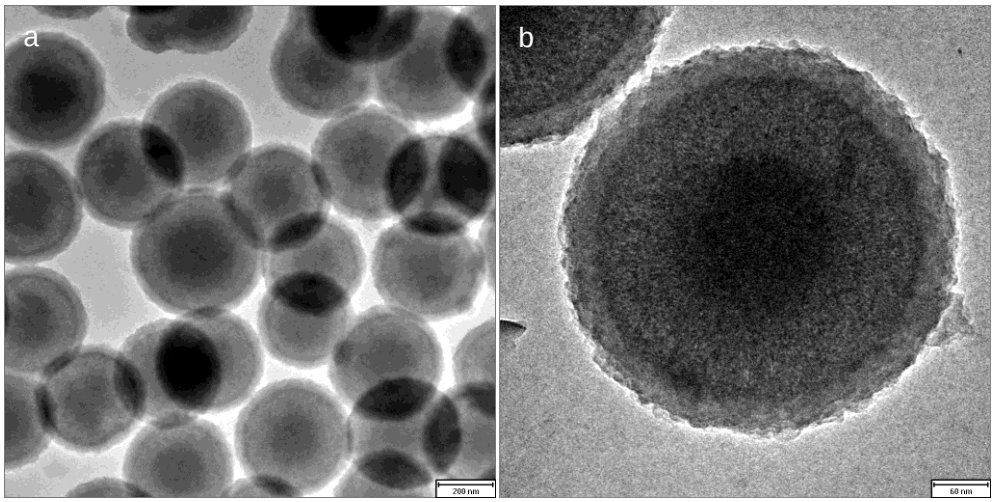


**Figure S17** (a,b) TEM images (at different magnifications) of Pt-*m*$SiO_2$@ZIF-8 intermediate collected after adding 2-MeIM for 1.5 h.

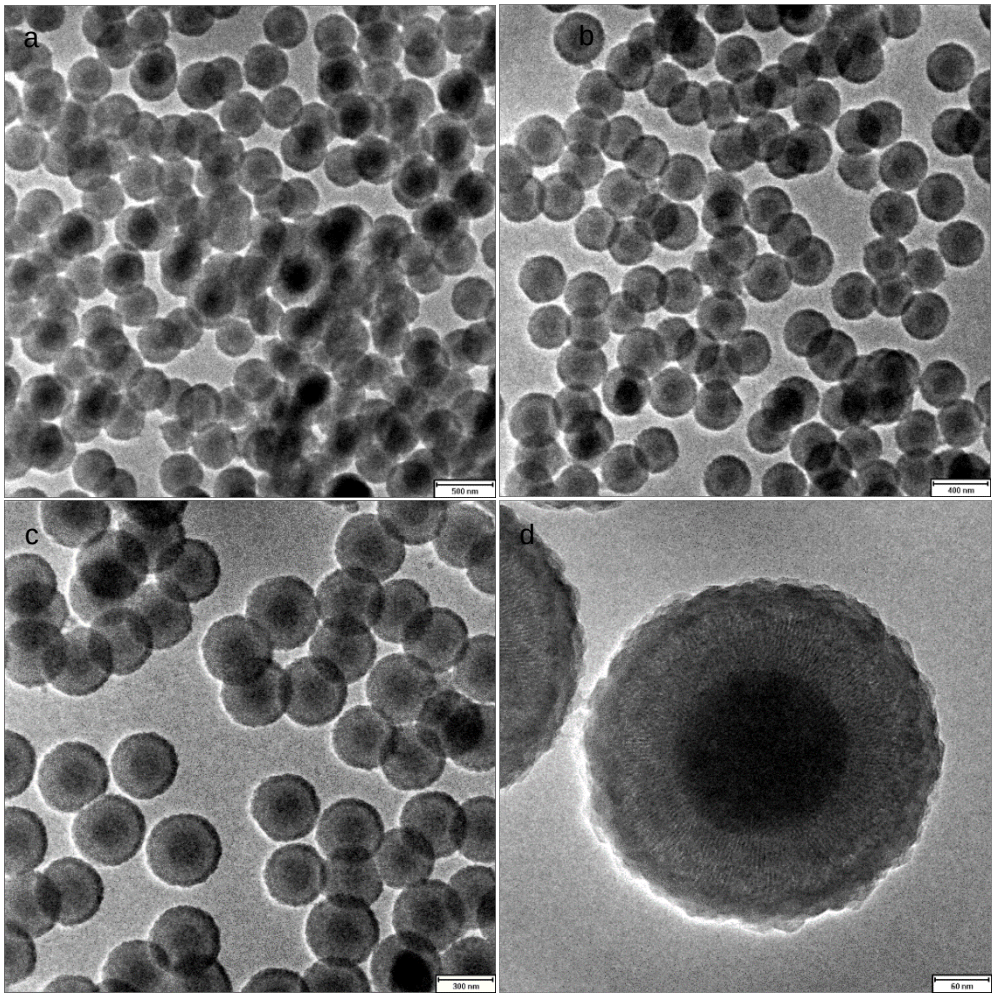


**Figure S18** TEM images (at different magnifications) of Pd-*m*$SiO_2$@ZIF-8 prepared with methanol as a solvent.

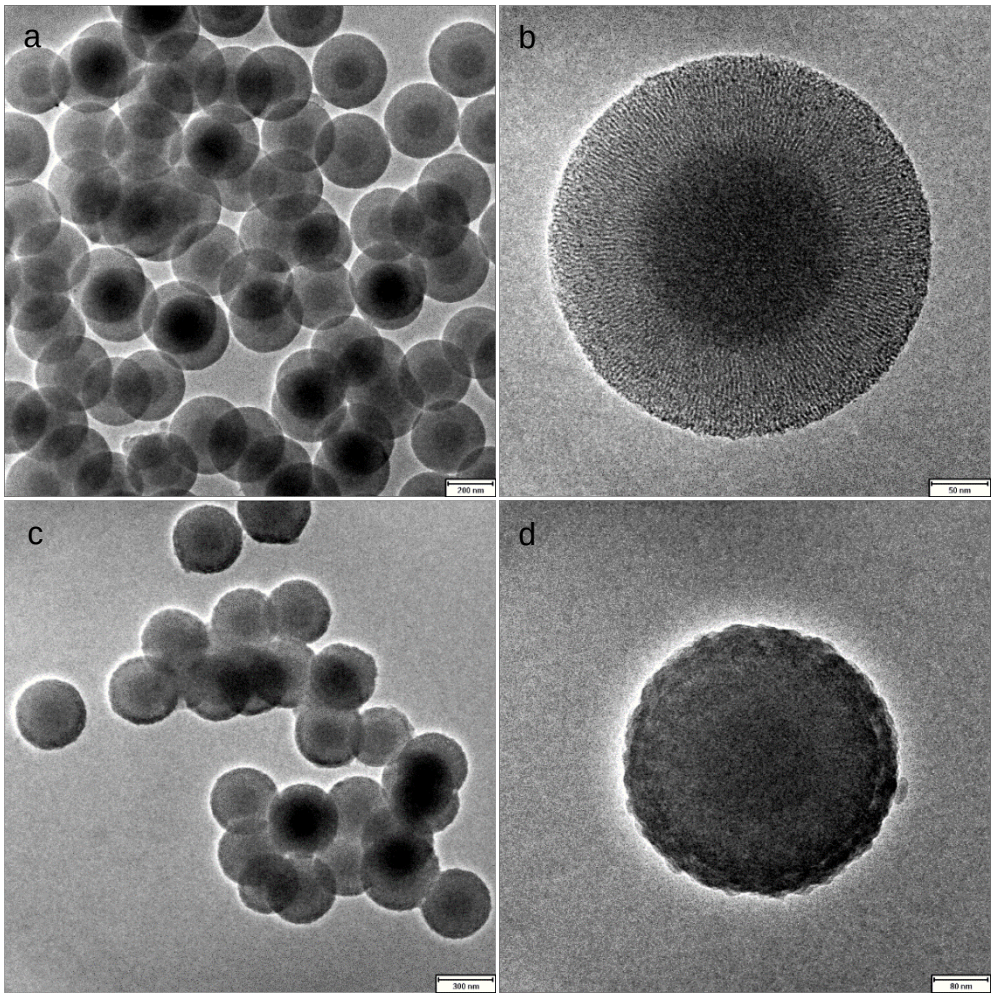


**Figure S19** TEM images (at different magnifications) of (a,b) Pd-*m*$SiO_2$ spheres and (c,d) Pd-*m*$SiO_2$@ZIF-8 composite spheres after catalytic hydrogenation reaction.